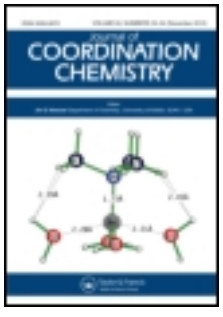

Journal of Coordination Chemistry
Publication details, including instructions for authors and subscription information:
http://www.tandfonline.com/loi/gcoo20

Syntheses, crystal structures, and DNA-binding of some nickel(II) complexes of 1,3-bis(2-pyridylmethylthio)propane and pseudohalides

Animesh Patra [a], Supriti Sen [a], Sandipan Sarkar [a], Ennio Zangrando [b] & Pabitra Chattopadhyay [a]

[a] Department of Chemistry, Burdwan University, Golapbag, Burdwan-713104, India

[b] Dipartimento di Scienze Chimiche e Farmaceutiche, Via Licio Giorgieri 1, 34127 Trieste, Italy

Accepted author version posted online: 21 Sep 2012.Published online: 11 Oct 2012.

To cite this article: Animesh Patra, Supriti Sen, Sandipan Sarkar, Ennio Zangrando & Pabitra Chattopadhyay (2012) Syntheses, crystal structures, and DNA-binding of some nickel(II) complexes of 1,3-bis(2-pyridylmethylthio)propane and pseudohalides, Journal of Coordination Chemistry, 65:23, 4096-4107, DOI: 10.1080/00958972.2012.732697

To link to this article: http://dx.doi.org/10.1080/00958972.2012.732697

Journal of Coordination Chemistry
Vol. 65, No. 23, 10 December 2012, 4096–4107

Syntheses, crystal structures, and DNA-binding of some nickel(II) complexes of 1,3-bis(2-pyridylmethylthio)propane and pseudohalides

ANIMESH PATRA†, SUPRITI SEN†, SANDIPAN SARKAR†, ENNIO ZANGRANDO‡ and PABITRA CHATTOPADHYAY*†

†Department of Chemistry, Burdwan University, Golapbag, Burdwan-713104, India
‡Dipartimento di Scienze Chimiche e Farmaceutiche, Via Licio Giorgieri 1, 34127 Trieste, Italy

(*Received 28 June 2012; in final form 30 August 2012*)

A series of neutral octahedral nickel(II) complexes of 1,3-bis(2-pyridylmethylthio)propane (L) and pseudohalide (X), formulated as $[Ni^{II}(L)X_2]$ (where X = azide (**1**), cyanate (**2**), and isothiocyanate (**3**)), was synthesized. The complexes were characterized by physico-chemical and spectroscopic methods, and **1** and **3** also by single-crystal X-ray diffraction analyses. The structural study shows nickel in a distorted octahedral geometry comprised of the tetradentate NSSN ligand with *trans* pyridines and monocoordinated pseudohalides in *cis* positions. In dimethylformamide solution, the complexes had quasi-reversible Ni^{II}/Ni^{III} redox couples in cyclic voltammograms with $E_{1/2}$ values of +0.732, +0.747, and +0.815 V for **1**, **2**, and **3**, respectively. To examine the biological activities of these complexes, interaction of **3** with calf thymus DNA was studied spectroscopically, showing groove-binding interaction.

Keywords: Nickel(II) complex; Crystal structure; DNA-binding study

1. Introduction

Geometrically distorted nickel(II) complexes with ligands having mixed N and S donors have received considerable attention due to nickel present in the active sites of several important classes of metalloproteins, either as homo- or hetero-dinuclear species. Prediction of the binding preference of polydentate ligands is still a challenge, especially when mixed donor species are involved. Complexes of nickel with nitrogen-based heterocyclic ligands have been widely investigated owing to their potential applications as functional solid materials, photosensitization reactions, bioinorganic chemistry, medicine, catalysis, and a variety of biological activities, such as antimalarial, antibacterial, antitumoral, and antiviral activities [1–6], which have often been related to the chelating ability of ligands toward trace metal ions.

Our interest in nitrogen–sulfur polydentate chelators [7, 8] is addressed toward their potential applications and we reported $NiCl_2$ and $FeCl_2$ complexes with tetradentate

*Corresponding author. Email: pabitracc@yahoo.com

ISSN 0095-8972 print/ISSN 1029-0389 online © 2012 Taylor & Francis
http://dx.doi.org/10.1080/00958972.2012.732697

1,3-bis(2-pyridylmethylthio)propane, L, having two pyridinic-N and two thioether-S donors [8]. Herein, we report Ni(II) complexes with the same L and with different coordinated pseudohalides. Structures of $[Ni(L)(N_3)_2]$ (**1**) and $[Ni(L)(SCN)_2]$ (**3**) have been established by single-crystal X-ray crystallography. Redox behavior of the complexes and binding study of **3** with calf thymus DNA (*ct*-DNA) are also described.

2. Experimental

2.1. *Materials and physical measurements*

All chemicals and reagents were obtained from commercial sources and used as received, unless otherwise stated. Solvents were distilled from an appropriate drying agent. 1,3-Bis(2-pyridylmethylthio)propane was synthesized following the procedure reported [8].

Elemental (C, H, and N) analyses were performed on a Perkin Elmer model 2400 elemental analyzer. Electronic absorption spectra were recorded on a JASCO UV-Vis/NIR spectrophotometer model V-570. Infrared (IR) spectra (KBr discs, 4000–300 cm^{-1}) were recorded using a Perkin-Elmer FTIR model RX1 spectrometer. Room-temperature magnetic susceptibility measurements were performed using a vibrating sample magnetometer PAR 155 model. Molar conductances (Λ_M) were measured in a Systronics Conductivity Meter 304 model using $\sim 10^{-3}$ mol L^{-1} solutions in appropriate organic solvents. Fluorescence spectra of ethidium bromide (EB) bound to DNA were obtained in a Hitachi-2000 fluorimeter. Electrochemical measurements were performed using computer-controlled CH-Instruments (Model No. CHI620D). All measurements were carried out under nitrogen at 298 K with reference to SCE electrode in DMSO using $[n\text{-}Bu_4N]ClO_4$ as supporting electrolyte.

2.2. *Preparation of the complexes*

The complexes were synthesized following a common procedure as described below. L (290.0 mg, 1.0 mmol) in methanol (10 mL) was added to a methanolic solution of nickel(II) acetate tetrahydrate (248.0 mg, 1.0 mmol) and the mixture was refluxed for 4 h. The resulting solution was cooled to ambient temperature and to this an aqueous solution of sodium azide (130 mg, 2.0 mmol) for **1**, or sodium cyanate (130 mg, 2.0 mmol) for **2**, or potassium thiocyanate (195 mg, 2.0 mmol) for **3**, was added with continuous stirring for 1 h. The crystallized product was collected from the solution on slow evaporation at room temperature after thorough washing with cold methanol and water and dried *in vacuo*. Single crystals of **1** and **3** suitable for X-ray analyses were obtained from methanolic solution of the crystallized products.

$[Ni(L)(N_3)_2]$ (**1**): $C_{15}H_8N_8S_2Ni$: Anal. Found: C, 41.82; H, 4.10; N, 25.72; Calcd: C, 41.60; H, 4.16; N, 25.88. IR (cm^{-1}): $\nu_{C=O}$, 1648; $\nu_{C=N}$, 1601; ν_{C-S}, 771, ν_{N3}, 2027. Magnetic moment (μ, B.M.): 3.08. Conductivity (Λ_o, $\Omega^{-1}\,cm^2\,mol^{-1}$) in DMF: 44. Yield 80–85%.

$[Ni(L)(NCO)_2]$ (**2**): $C_{17}H_{18}N_4S_2O_2Ni$: Anal. Found: C, 47.64; H, 4.18; N, 13.28; Calcd: C, 47.15; H, 4.16; N, 12.94. IR (cm^{-1}): $\nu_{C=O}$, 1648; $\nu_{C=N}$, 1601; ν_{C-S}, 771, ν_{NCO}, 2182.

Magnetic moment (μ, B.M.): 3.10. Conductivity (Λ_o, $\Omega^{-1}\,cm^2\,mol^{-1}$) in DMF: 48. Yield 75–80%.

[Ni(L)$(SCN)_2$] (**3**): $C_{17}H_{18}N_4S_4Ni$: Anal. Found: C, 43.98; H, 3.90; N, 12.04; Calcd: C, 43.90; H, 3.87; N, 12.05. IR (cm^{-1}): $\nu_{C=O}$, 1648; $\nu_{C=N}$, 1601; ν_{C-S}, 771, ν_{NCS}, 2082. Magnetic moment (μ, B.M.): 3.06. Conductivity (Λ_o, $\Omega^{-1}\,cm^2\,mol^{-1}$) in DMF: 42. Yield 80–85%.

2.3. *DNA-binding experiments*

The *ct*-DNA used in the experiments was sufficiently free from protein as the ratio of UV absorbance of solutions of DNA in tris-HCl at 260 and 280 nm (A_{260}/A_{280}) was almost ≈ 1.9. Stock solution of DNA was always stored at 4°C and used within 4 days. Stock solution of the Ni(II) complex was prepared by dissolving the complex in DMSO and suitably diluted with tris-HCl buffer to the required concentration. Absorption spectral titration experiment was performed by keeping the concentration of the Ni(II) complex constant. Fluorescence displacement was carried out in the presence of EB. The solution of the Ni(II) complex was titrated into the saturated bound DNA/EB mixture. Before measurements, the mixture was shaken and incubated at room temperature for 30 min. The fluorescence spectra of EB bound to DNA were obtained at an emission wavelength of 522 nm in the Fluorimeter (Hitachi-2000).

2.4. *X-ray crystal structure analysis*

Diffraction data collections of **1** and **3** were carried out at room temperature on a Nonius DIP-1030H system by using Mo-Kα radiation ($\lambda = 0.71073$ Å). Cell refinement, indexing and scaling of the data sets were performed using Denzo and Scalepack [9]. Both the structures were solved by direct methods and subsequent Fourier analyses and refined by full-matrix least-squares based on F^2 with all observed reflections [10]. Hydrogen atoms were fixed at geometrical positions. Restraints were applied on thermal parameters of the C7–C8–C9 bridge moiety of **1**, due to a local disorder. All calculations were performed using the WinGX System, Ver 1.80.05 [11]. Details of the crystal data and structure refinements for **1** and **3** are given in table 1.

3. Results and discussion

3.1. *Synthesis and characterization*

The ligand 1,3-bis(2-pyridylmethylthio)propane, L, was synthesized by the reaction of propanedithiol with 2-picolyl chloride in the presence of sodium ethoxide. The complexes were obtained in good yield from the reaction of nickel(II) acetate tetrahydrate with equimolar amount of L in methanol and corresponding aqueous solution of twice molar quantity of pseudohalides (scheme 1). L is a tetradentate neutral ligand through N_2S_2 donors. All monomeric complexes are soluble in common organic solvents. The μ values at room temperature of these complexes are 3.08 (**1**), 3.10 (**2**), and 3.06 BM (**3**), which indicate high-spin octahedral complexes. The conductivity of

Table 1. Crystallographic data for **1** and **3**.

	1	**3**
Empirical formula	$C_{15}H_{18}N_8NiS_2$	$C_{17}H_{18}N_4NiS_4$
Formula weight	433.20	465.30
Crystal size (mm^3)	$0.40 \times 0.40 \times 0.12$	$0.35 \times 0.35 \times 0.15$
Crystal system	Monoclinic	Monoclinic
Space group	$P\ 2_1/n$	$P\ 2_1/c$
Unit cell dimensions (Å, °)		
a	10.229(3)	7.870(2)
b	11.446(3)	14.013(3)
c	15.979(3)	18.708(4)
β	91.76(3)	91.89(2)
Volume ($Å^3$), Z	1870.0(8), 4	2062.0(8), 4
Calculated density ($g\,cm^{-3}$)	1.539	1.499
$F(000)$	896	960
θ Range (°)	2.55–25.34	1.82–26.37
Absorption coefficient (Mo-Kα) (mm^{-1})	1.278	1.355
Collected reflection	6046	24,717
Independent reflection	3167	4011
R int	0.025	0.0557
Observed data [$I > 2\sigma(I)$]	1617	2154
Parameters	235	235
R_1, wR_2 [$I > 2\sigma(I)$]	0.0421, 0.1006	0.0396, 0.0963
R_1, wR_2	0.0814, 0.1111	0.0764, 0.1053
Goodness-of-fit on F^2	0.830	0.822
Residuals ($e\,Å^{-3}$)	0.527 and −0.353	0.343 and −0.357

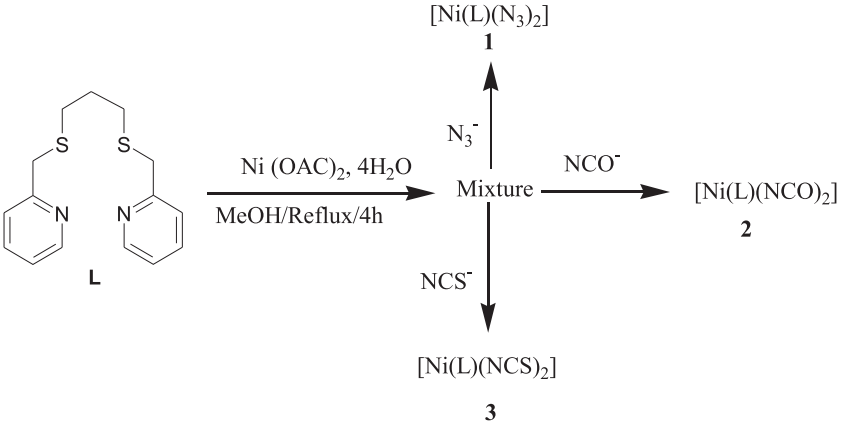

Scheme 1. Synthetic strategy for **1–3**.

these complexes in DMF shows conductance values of 42–48 (Λ_o, $\Omega^{-1}\,cm^2\,mol^{-1}$), suggesting non-electrolytes.

3.2. *Structures of 1 and 3*

The molecular structures of **1** and **3** with atom-numbering schemes are shown in figures 1 and 2, respectively, and a selection of bond lengths and angles is reported in table 2. The X-ray crystal structure analyses confirm the formation of neutral complexes where

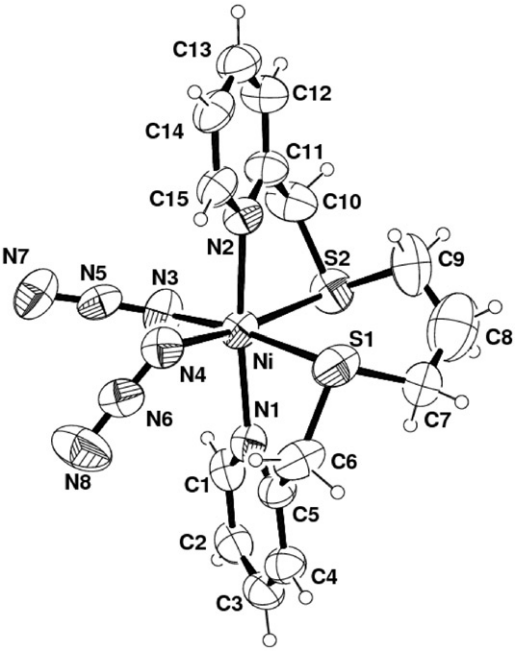

Figure 1. ORTEP view of **1** with atom-labeling scheme.

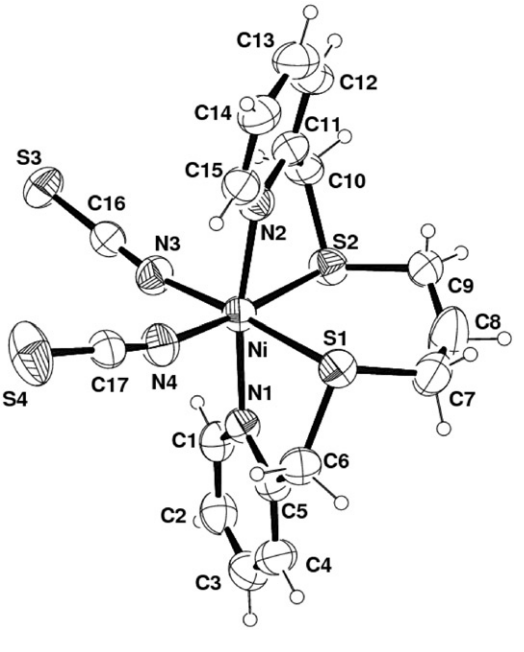

Figure 2. ORTEP view of **3** with atom-labeling scheme.

Table 2. Selected bond distances (Å) and angles (°) for **1** and **3**.

	1	**3**
Ni–S(1)	2.4604(14)	2.4542(11)
Ni–S(2)	2.4329(15)	2.4312(11)
Ni–N(1)	2.092(4)	2.097(3)
Ni–N(2)	2.079(4)	2.097(3)
Ni–N(3)	2.048(4)	2.046(3)
Ni–N(4)	2.037(4)	2.031(3)
S(1)–Ni–S(2)	92.87(6)	96.56(4)
S(1)–Ni–N(1)	80.76(11)	82.23(8)
S(1)–Ni–N(2)	95.29(11)	90.61(8)
S(1)–Ni–N(3)	172.80(14)	176.50(9)
S(1)–Ni–N(4)	86.41(13)	85.43(10)
S(2)–Ni–N(1)	94.79(11)	92.09(8)
S(2)–Ni–N(2)	80.86(11)	81.99(9)
S(2)–Ni–N(3)	86.76(13)	86.02(9)
S(2)–Ni–N(4)	171.90(13)	175.20(9)
N(1)–Ni–N(2)	174.02(13)	170.17(10)
N(1)–Ni–N(3)	92.10(17)	95.34(12)
N(1)–Ni–N(4)	93.06(16)	92.50(12)
N(2)–Ni–N(3)	91.75(17)	92.09(12)
N(2)–Ni–N(4)	91.17(17)	93.65(12)
N(3)–Ni–N(4)	94.96(17)	92.18(13)

nickel(II) is coordinated by the tetradentate L by NSSN donors. The ligand binds such that pyridines are *trans*, while the two thioether donors are located in the equatorial plane with two azides (in **1**) and thiocyanates (in **3**). The monodentate *cis* pseudohalides complete the distorted octahedral coordination sphere.

The configuration of L is comparable in the two complexes although distortions are evident in the coordination geometry (see figures 1 and 2). The same coordination pattern of L was also detected in $[NiLCl_2]$ and $[FeLCl_2]$ derivatives [8]. In the present complexes, the Ni–N(py) bond distances (range 2.079(4)–2.097(3) Å) are slightly longer than the Ni–N(pseudohalide) ones that vary from 2.031(3) to 2.048(4) Å, while the Ni–S bond lengths fall between 2.4312(11) and 2.4604(14) Å. Coordination bond angles deviate from ideal octahedral geometry; the more evident are N(1)–Ni–N(2) angles of 174.02(13)° and 170.17(10)° in **1** and **3**, respectively, which confirm the strain of the ligand on coordination. All these data compare well with those found in the $[NiLCl_2]$ species [8]. While Ni–N (N_3 or NCS) are comparable within $\pm 2\sigma$, indicating comparable bond strength, it is worth noting the different values measured at the N donor of N_3^- and SCN^-; in **1** the N–N–Ni bond angle is *ca* 122°, while in **3** the C–N–Ni values average to 164.2°, showing a more linear coordination.

3.3. *Spectral studies*

The IR spectra of all the complexes exhibit characteristic strong to medium intensity bands at 1468–1472 and 758–762 cm^{-1}, assignable to $\nu_{C=N}$ and ν_{C-S}, respectively, along with other characteristic bands. Intense bands at 2027 cm^{-1} for **1**, 2182 cm^{-1} for **2**, and 2082 cm^{-1} for **3** are assignable to ν_{N3}, ν_{NCO}, and ν_{NCS}, respectively [12]. These IR data confirm the presence of end-on N-bonded terminal pseudohalides [13, 14].

Table 3. UV-Vis spectral and electrochemical data.

Compound	UV-Vis data[a] λ, nm (ε, $dm^3 mol^{-1} cm^{-1}$)	Electrochemical data[a,b] E_{pc} (V)	E_{pa} (V)	$E_{1/2}$, ΔE (V)	Reversibility (I_{pc}/I_{pa})
1	245(3012), 267(45,682), 339(516), 450(131)	+0.644	+0.820	+0.732 (176)	1.02
2	234(2303), 264(18,864), 346(4898), 370(109)	+0.668	+0.826	+0.747 (158)	0.95
3	240(2715), 267(42,778), 345(607), 530(33)	+0.733	+0.897	+0.815 (164)	0.91

$E_{1/2} = (E_{pc} + E_{pa})/2$; I_{pc}/I_{pa} is constant for scans in the range of 50–400 mV s^{-1}.
[a]In DMF.
[b]Data recorded in mV, at 298 K and scan rate 100 mV s^{-1}.

Electronic absorption spectra of **1**–**3** were recorded at room temperature using DMF as solvent and the data are tabulated in table 3. All spectra of complexes have bands lower than 400 nm due to intramolecular $\pi \rightarrow \pi^*$ and $n \rightarrow \pi^*$ transitions for the aromatic ring. In octahedral nickel(II) complexes, three spin-allowed transitions are expected from the energy level diagram for d^8 ions due to $^3A_{2g} \rightarrow {}^3T_{1g}$ (P), $^3A_{2g} \rightarrow {}^3T_{1g}$ (F), and $^3A_{2g} \rightarrow {}^3T_{2g}$ transitions, observed from low to high wavelengths, respectively. Bands at 450 and 530 nm may be assigned to $^3A_{2g} \rightarrow {}^3T_{1g}$ (P) (in **1** and **2**) and $^3A_{2g} \rightarrow {}^3T_{1g}$ (F) (in **3**) transitions, respectively. The peak of very low intensity at 850 nm is due to the $^3A_{2g} \rightarrow {}^3T_{2g}$ transition. These observations suggest an octahedral geometry of Ni(II).

3.4. *DNA-binding studies*

The binding interaction of metal complexes (not only of nickel) with different ligands has been investigated [15–19]. Due to structural similarity of the present complexes, only the behavior of **3** with *ct*-DNA was tested by using absorption and emission spectra. Electronic absorption spectroscopy is an effective method to examine the binding modes of metal complexes with DNA. Binding of the nickel(II) complex to *ct*-DNA helix is examined by an increase in the absorption (*ca* 265 nm) of nickel(II). This increase indicates involvement of a strong interaction between the complex and the base pairs of DNA [20]. Absorption spectra of **3** in the absence and presence of *ct*-DNA are given in figure 3. The extent of the hyperchromism in the charge-transfer band is generally consistent with the strength of interaction [21–24]. The binding strength of the complex with *ct*-DNA, as measured by the intrinsic binding constant K_b, was determined from the spectral titration data using equation (1) [25]:

$$[DNA]/(\varepsilon_a - \varepsilon_f) = [DNA]/(\varepsilon_b - \varepsilon_f) + 1/[K_b(\varepsilon_b - \varepsilon_f)], \quad (1)$$

where [DNA] is the concentration of DNA, ε_f, ε_a, and ε_b correspond to extinction coefficients, respectively, for the free complex, for each addition of DNA to the complex and for the metal complex in the fully bound form. A plot of $[DNA]/(\varepsilon_a - \varepsilon_f)$ *versus* [DNA] (figure 4) gives K_b, the intrinsic binding constant as the ratio of slope to the intercept. From the $[DNA]/(\varepsilon_a - \varepsilon_f)$ *versus* [DNA] plot, the binding constant K_b for **3** was estimated to be $1.07 \times 10^5 (mol\,L^{-1})^{-1}$ ($R = 0.9941$ for five points), which is comparable

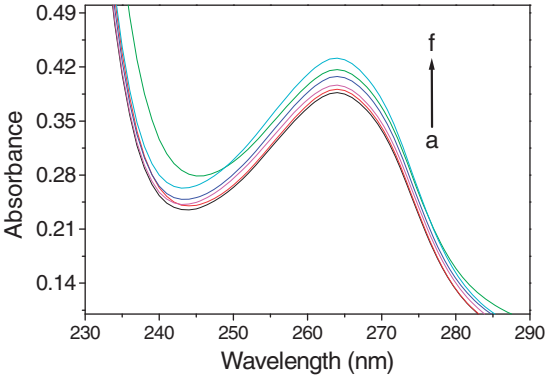

Figure 3. Electronic spectral titration of **3** with *ct*-DNA at 266 nm in tris-HCl buffer. [**3**] = 1.31×10^{-5} mol L^{-1}; [DNA]: (a) 0.0, (b) 2.0×10^{-6}, (c) 4.00×10^{-6}, (d) 6.0×10^{-6}, (e) 8.0×10^{-6}, and (f) 1.0×10^{-5} mol L^{-1}. The increase in DNA concentration is indicated by an arrow.

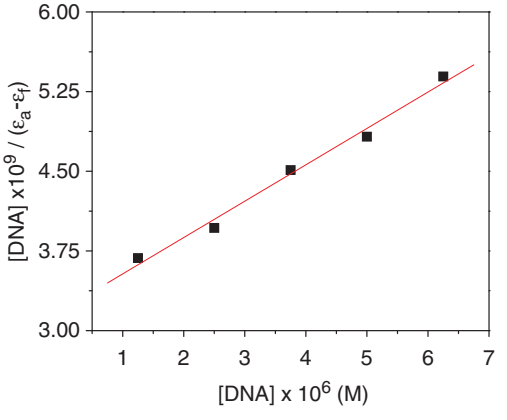

Figure 4. Plot of [DNA]/($\varepsilon_a - \varepsilon_f$) *vs.* [DNA] for the absorption titration of *ct*-DNA with **3** in tris-HCl buffer ($R = 0.9941$ for five points).

to those of some DNA intercalation Ni(II) complexes (0.85–0.88 $\times 10^5$ (mol L^{-1})$^{-1}$) [26] and lower than some DNA intercalation Ni(II) complexes [15–17].

Fluorescence intensity of EB bound to DNA at 522 nm shows a decreasing trend with the increasing concentration of **3** (figure 5). The spectrum indicated by "f" (pink line in figure 5) clearly points out the maximum binding of nickel(II) complex with *ct*-DNA by replacing EB. The quenching of EB bound to DNA by the nickel(II) complexes are in agreement with the linear Stern–Volmer equation (2) [27]:

$$I_0/I = 1 + K_{sv}[Q], \tag{2}$$

where I_0 and I represent the fluorescence intensities in the absence and presence of quencher, respectively, K_{sv} is a linear Stern–Volmer quenching constant, and Q is the concentration of quencher. In the quenching plot (figure 6) of I_0/I *versus* [complex], K_{sv} is calculated to be 0.69×10^4, also indicating a strong groove-binding interaction of the

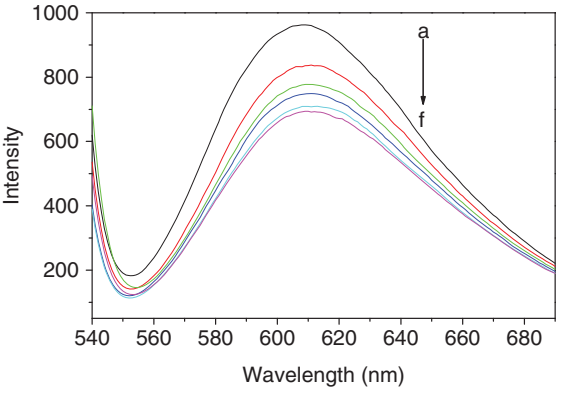

Figure 5. Emission spectra of the *ct*-DNA-EB system in tris-HCl buffer during the titration of **3** ($\lambda_{ex} = 522$ nm). The arrow shows the intensity change by increasing the complex concentration.

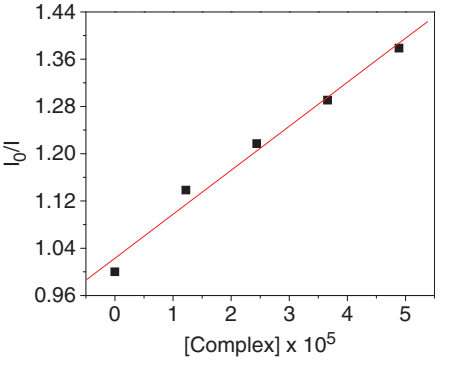

Figure 6. Plot of I_0/I *vs.* [complex] for the titration of **3** with *ct*-DNA-EB system in tris-HCl buffer ($R = 0.99179$ for five points).

nickel(II) complex with *ct*-DNA. The K_{sv} value is comparable with Ni(II) complex ($7.3 \times 10^3 (\text{mol L}^{-1})^{-1}$) [19] and lower than another Ni(II) complex ($5.92 \times 10^4 (\text{mol L}^{-1})^{-1}$) [27].

The titration data obtained from the fluorescence experiment can also be helpful for calculating the number of binding sites and apparent binding constant using equation (3) [28]:

$$\log[(I_0 - I)/I] = \log K + n \log[\text{complex}], \tag{3}$$

where K and n are the binding constant and number of binding site(s) of the complex with *ct*-DNA. The number of binding sites (n) determined from the intercept of $\log[(I_0 - I)/I]$ *versus* log[complex] is 0.65, indicating a lower association of **3** to the number of DNA bases through only a single-binding site. Thus the value suggests strong affinity of **3** through surface or groove-binding. The calculated value of the equilibrium binding constant K, of 0.1×10^4, is in fair agreement with the value of the

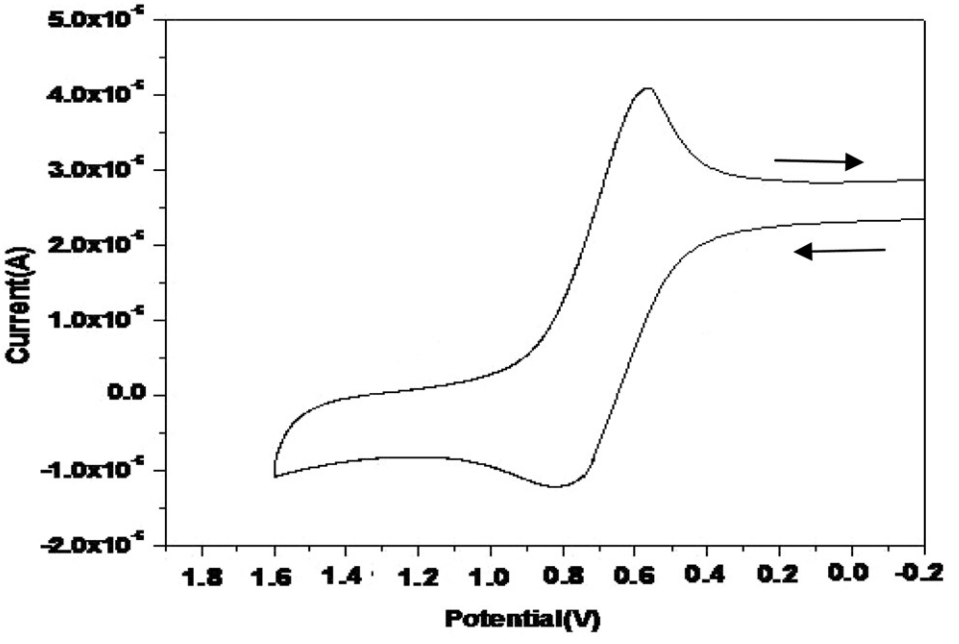

Figure 7. A representative cyclic voltammogram of [Ni(L)N_3] complex (**1**) showing quasi-reversible Ni^{II}/Ni^{III} redox couple in DMF having [*n*-Bu_4N]ClO_4 (0.1 mol L^{-1}) as a supporting electrolyte at 298 K (scan rate of 100 mV s^{-1}).

apparent binding constant calculated from absorption spectroscopy, and comparable to that of 1.65×10^4 reported for a nickel complex with a tetradentate Schiff base [16]. However, since the NSSN ligand differs from the typical Schiff bases of Ni complexes interacting with DNA reported in the literature [15–19], a comparison of our results with those published is not straightforward, also different techniques are used.

3.5. *Electrochemistry*

Redox properties of the complexes were examined by cyclic voltammetry using a Pt-disc working electrode and a Pt-wire auxiliary electrode in dry DMF using [*n*-Bu_4N]ClO_4 (0.1 mol L^{-1}) as the supporting electrolyte (figure 7). Voltammetric data are given in table 3. The cyclic voltammograms exhibit quasi-reversible Ni^{II}/Ni^{III} redox couples in DMF and the $E_{1/2}$ values (*versus* Ag/AgCl at 298 K) were +0.732, +0.747, and +0.815 V for **1**, **2**, and **3**, respectively. Here, the $E_{1/2}$ value for **3** lies at the relatively higher anodic side of the range generally measured, 0.3–0.8 V, for the Ni^{II}/Ni^{III} oxidation potential data for thioether containing nickel(II) complexes [29], indicating that Ni^{II} is stabilized in **3**, perhaps due to the presence of the soft isothiocyanate compared to azide and cyanate, or to the chloride coligand in a previous study [8]. No cathodic response for $Ni^{II} \rightarrow Ni^{I}$ reduction was obtained for the complexes up to −1.50 V. The voltammetric parameters were studied in the scan rate interval 50–400 mV s^{-1}. The ratio between the cathodic peak current and the square root of the

scan rate ($I_{pc}/\nu^{1/2}$) is approximately constant. The peak potential shows a small dependence on the scan rate. The ratio I_{pc} to I_{pa} is close to unity. From these data, the redox couple is related to a quasi-reversible one-electron transfer process controlled by diffusion.

4. Conclusion

Three new mononuclear octahedral nickel(II) complexes with a ligand having a NSSN donor set and with pseudohalides (azide, cyanate, and thiocyanate) have been synthesized and structurally characterized. The single-crystal X-ray diffraction study of the azide and thiocyanate derivatives indicates comparable coordination for the tetradentate ligand with pseudohalides occupying *cis* positions. The interaction of the Ni(II) complexes with *ct*-DNA at physiological pH shows very good agreement between spectrophotometric and fluorimetric methods of measurement. The data lend support to the validity of the methods and compare to the binding mode of the reported Ni(II) complexes with *ct*-DNA [15–19, 26].

Supplementary material

Crystallographic data for the structural analyses have been deposited with the Cambridge Crystallographic Data Centre, CCDC Nos 861488 and 861489 for **1** and **3**, respectively. Copies of this information are available on request, free of charge, from CCDC, 12 Union Road, Cambridge, CB2 1EZ, UK (Fax: +44-1223-336-033; E-mail: deposit@ccdc.ac.uk or http://www.ccdc.cam.ac.uk).

Acknowledgments

Financial support from the Department of Science and Technology, New Delhi, India is gratefully acknowledged.

References

[1] X.-H. Zhou, T. Wu, D. Li. *Inorg. Chim. Acta*, **359**, 1442 (2006).
[2] R.M. Kretzer, R.A. Ghiladi, E.L. Lebeau, H.-C. Liang, K.D. Karlin. *Inorg. Chem.*, **42**, 3016 (2003).
[3] C. Marzano, M. Pellei, D. Colavito, S. Alidori, G.G. Lobbia, V. Gandin, F. Tisato, C. Santini. *J. Med. Chem.*, **49**, 7317 (2006).
[4] E.I. Solomon, P.M. Jones, J.A. Maj. *Chem. Rev.*, **93**, 2623 (1993).
[5] J.S. Casas, E.E. Castellans, M.D. Louce, J. Ellena, A. Sanchez, J. Sordo, C. Taboada. *J. Inorg. Biochem.*, **11**, 1858 (2006).
[6] Y.P. Tian, C.Y. Duan, Z.L. Lu, X.Z. You, H.K. Fun, S. Kandasamy. *Polyhedron*, **15**, 2263 (1996).
[7] S. Sarkar, S. Sen, S. Dey, E. Zangrando, P. Chattopadhyay. *Polyhedron*, **29**, 3157 (2010), and references therein.
[8] A. Patra, S. Sarkar, M.G.B. Drew, E. Zangrando, P. Chattopadhyay. *Polyhedron*, **28**, 1261 (2009).

[9] Z. Otwinowski, W. Minor. In *Methods in Enzymology*, C.W. Carter Jr, R.M. Sweet (Eds), Vol. 276, p. 307, Academic Press, New York (1997).
[10] G.M. Sheldrick. *Acta Cryst. A*, **64**, 112 (2008).
[11] L.J. Farrugia. *J. Appl. Crystallogr.*, **32**, 837 (1999).
[12] A.R. Davis, C.J. Murphy, R.A. Plane. *Inorg. Chem.*, **9**, 1081 (1970).
[13] M. Habib, T.K. Karmakar, G. Aromı, J.R. Arino, H.-K. Fun, S. Chantrapromma, S.K. Chandra. *Inorg. Chem.*, **47**, 4109 (2008).
[14] K. Nakamoto. *Infrared and Raman Spectra of Inorganic and Coordination Complexes*, 4th Edn, Wiley, New York, NY (1992).
[15] P.S. Guin, P.C. Mandal, S. Das. *J. Coord. Chem.*, **65**, 705 (2012).
[16] N. Raman, K. Pothiraj, T. Baskaran. *J. Coord. Chem.*, **64**, 4286 (2011).
[17] N. Raman, K. Pothiraj, T. Baskaran. *J. Coord. Chem.*, **64**, 3900 (2011).
[18] M. Manjunatha, V.H. Naik, A.D. Kulkarni, S.A. Patil. *J. Coord. Chem.*, **64**, 4264 (2011).
[19] M. Shakir, S. Khanam, M. Azam, M. Aatif, F. Firdaus. *J. Coord. Chem.*, **64**, 3158 (2011).
[20] A. Ambroise, B.G. Maiya. *Inorg. Chem.*, **39**, 4264 (2000).
[21] S.A. Tysoe, R.J. Morgan, A.D. Baker, T.C. Strekas. *J. Phys. Chem.*, **97**, 1707 (1993).
[22] J.K. Barton, A.T. Danishefsky, J. Goldberg. *J. Am. Chem. Soc.*, **106**, 2172 (1984).
[23] J.M. Kelly, A.B. Tossi, D.J. McConnell, C. OhUigin. *Nucleic Acid Res.*, **13**, 6017 (1985).
[24] R. Vijayalakshmi, M. Kanthimathi, V. Subramanian, B.U. Nair. *Biochem. Biophys. Acta*, **1475**, 157 (2000).
[25] A.M. Pyle, J.P. Rehmann, R. Meshoyrer, C.V. Kumar, N.J. Turro, J.K. Barton. *J. Am. Chem. Soc.*, **111**, 3051 (1989).
[26] J. Xu, Y. Chen, H. Zhou, Z. Pan. *J. Coord. Chem.*, **64**, 1626 (2011).
[27] O. Stern, M. Volmer. *Z. Phys.*, **20**, 183 (1919).
[28] A. Kathiravan, R. Renganathan. *Polyhedron*, **28**, 1374 (2009).
[29] S. Karmakar, S.B. Choudhury, D. Ray, A. Chakravorty. *Polyhedron*, **12**, 291 (1993).